Differential effects of inhibitory G-protein isoforms on G-protein gated inwardly rectifying K^+ currents in adult murine atria

Muriel Nobles[1], David Montaigne[2], Sonia Sebastian[1], Lutz Birnbaumer[3] and Andrew Tinker[1*]

[1] The Heart Centre, William Harvey Research Institute, Barts and the London School of Medicine and Dentistry, Charterhouse Square, London, EC1M6BQ, UK

[2] CHU Lille, France, Université Lille 2, F-59000 Lille, France; Inserm, U1011, F-59000 Lille, France; EGID, F-59000 Lille, France; Institut Pasteur de Lille, F-59019 Lille, France.

[3] Division of Intramural Research, National Institute of Environmental Health Sciences, Research Triangle Park, NC 27709, USA and the Institute of Biomedical Research (BIOMED), Catholic University of Argentina, C1107AFF Buenos Aires, Argentina.

* Author for correspondence e-mail: a.tinker@qmul.ac.uk Tel: 020 7882 5783

Abstract

G-protein gated inwardly rectifying K^+ (GIRK) channels are the major inwardly rectifying K^+ currents in cardiac atrial myocytes and an important determinant of atrial electrophysiology. Inhibitory G-protein alpha subunits can both mediate activation via acetylcholine but can also supress basal currents in the absence of agonist. We studied this phenomenon using whole cell patch clamping in murine atria from mice with global genetic deletion of $G\alpha_{i2}$, combined deletion of $G\alpha_{i1}/G\alpha_{i3}$ and littermate controls. We found that mice with deletion of $G\alpha_{i2}$ had increased basal and agonist activated currents particularly in the right atria whilst in contrast those with $G\alpha_{i1}/G\alpha_{i3}$ deletion had reduced currents. Mice with global genetic deletion of $G\alpha_{i2}$ had decreased action potential duration. Tissue preparations of the left atria studied with a multielectrode array from $G\alpha_{i2}$ knockout mice showed a shorter effective refractory period, with no change in conduction velocity, than littermate controls. Transcriptional studies revealed increased expression of GIRK channel subunit genes in $G\alpha_{i2}$ knockout mice. Thus different G-protein isoforms have differential effects on GIRK channel behaviour and paradoxically $G\alpha_{i2}$ acts to increase basal and agonist activated GIRK currents. Deletion of $G\alpha_{i2}$ is potentially proarrhythmic in the atria.

Keywords: atria, electrophysiology, inhibitory heterotrimeric G-protein, G-protein gated potassium channel

Running Title: Inhibitory G-proteins and atrial electrophysiology

Introduction

Inwardly rectifying K+ channels are widely expressed in all chambers of the heart and are important in setting the resting membrane potential. However there is a dichotomy with the Kir2.0 family being predominant in the ventricles and His-Purkinje system and the Kir3.0 family in atrial and nodal tissues (7; 18; 24; 45). The Kir3.0 channel family encodes G-protein gated inwardly rectifying K+ channel present in neurons and neuroendocrine tissues in addition to the heart (11; 27). In the heart the channel is thought to consist largely of a heteromultimer of Kir3.1 and Kir3.4 (19). A characteristic of these channels is that they are activated by G-protein coupled receptors linked to inhibitory G-proteins and specifically by the free Gβγ subunits (25; 42; 44). For example, in the sinoatrial node activation of the channel by acetylcholine released from the vagus nerve is responsible for heart rate slowing (39; 43). Recently a study has shown a critical role for Kir3.4 in the kinetics of heart rate recovery to resting level after sympathetic activation (30).

Despite GIRK channel activation being mediated by Gβγ directly binding to domains on the channel, activation seems to occur largely via members of the inhibitory G-protein family (14; 21; 22; 35). In a series of studies from different laboratories using varied approaches a more complex model has emerged. It appears that the inhibiory G-protein heterotrimer is able to directly interact with channel and on activation heterotrimer dissociation occurs in a microdomain in or around the channel subunit. The dissoicated Gβγ subunit leads to activation (9; 21; 34; 38). However the Gα as either a monomer or as part of the heterotrimer may also play an important role leading to inhibition of channel activity and this process may be isoform dependent (5; 6; 15). Multiple isoforms of inhibitory Gα subunits ($G\alpha_{i1}$, $G\alpha_{i2}$, $G\alpha_{i3}$ and, $G\alpha_{o}$) are present in atrial tissue, and their roles in modulating parasympathetic signal transduction remain unclear. The subunits $G\alpha_{i2}$, $G\alpha_{i3}$ have been

shown to mediate signaling to GIRK in embryonic stem cell derived cardiomyocytes (Sowell et al., 1997). Our own work shows that $G\alpha_{i2}$ is important for heart rate regulation *in-vivo* (41; 46) but this occurs via modulation in the SA node (not the atria) and might be via a mechanism independent of GIRK.

There is further complexity in that the right and left atria may be different and have gradients of channel expression (17). GIRK channels are expressed at higher levels in the right atrium in mice and humans. It has been proposed that the gradient of GIRK current, combined with the heterogenous distribution of parasympathetic innervation and adenosine receptor expression in the atria, may contribute to the ability of vagal nerve stimulation to augment dispersion of atrial refractoriness (12; 13; 23; 26; 40). The purpose of this study is to define the type of G-proteins involved in the signalling to GIRK in the atria, the possible role of these G-proteins in atrial asymmetry and how they might potentially modulate arrhythmogenesis.

Material and Methods

Gene-targeted mice

Mice with global deletion of $G\alpha_{i2}$, and $G\alpha_{i1}/G\alpha_{i3}$ (deletion of both $G\alpha_{i1}$ and $G\alpha_{i3}$) maintained on a Sv129 background were compared with wild-type littermate controls. The gene-targeting strategy, genotyping and confirmation of relevant $G\alpha_{i/o}$ deletions have previously been described (16; 46). Mice were maintained in an animal core facility under the UK Home Office guidelines relating to animal welfare. All procedures were approved by the local animal care and use committee and performed in accord with the UK Home Office regulations (PPL 70\7665). All mice were kept in a temperature controlled environment (21-24°C) with 12/12hr light/dark cycle. Animals were allowed ad-libitum access to standard rodent chow and drinking water. Mice aged 3–4 months were used for this study. Littermate controls were obtained from the $G\alpha_{i2}$ crosses.

Quantitative real time reverse transcriptionPCR

RNA was isolated from the left atria and right atria from mice with global deletion of $G\alpha_{i2}$, maintained on a Sv129 background and, wild-type littermate controls using the RNeasy kit (Qiagen). Briefly, hearts were removed from each group of mice ($G\alpha_{i2}$ (+/+) and, $G\alpha_{i2}$(-/-)), washed with cold PBS, left atria and right atria were isolated and immediately placed in RNA Later. RNA was extracted using RNeasy kit (cat no. 74104 Qiagen). cDNA was synthesized using the High capacity cDNA reverse transcription Kit (4368814 Life technologies) quantified and 50ng of cDNA/20µl was used for the subsequent real time expression assay. Real-time PCR was performed using Taqman gene expression Assays (Life technologies). All genes (Mm00434618_m1**:** Kcnj3, Mm01175829_m1**:** Kcnj5, Mm00492379_m1**:** Gnai3, Mm01165301_m1**:** Gnai1, Mm00494677_m1**:** Gnb1,

Mm00501973_m1: Gnb4, Mm01165191_m1: Gng11, Mm00515876_m1: Gng7) were assayed in triplicates and GAPDH was used as the house keeping gene.

Single-cell isolation and electrophysiology

Atrial and sinoatrial cells were isolated using an adapted method for isolation of sinoatrial cardiomyocytes (29). Briefly, mice were injected with heparin and beating hearts were removed under pentobarbital (3 ml/kg) and ketamine (1 ml/kg) anaesthesia. The left and right atria were excised in normal Tyrode solution containing (mM): NaCl, 140; KCl, 5.4; $CaCl_2$, 1.8; $MgCl_2$, 1; Hepes–NaOH, 5; and D-glucose, 5.5; (pH 7.4). Strips of tissues were enzymatically digested in a low-Ca^{2+} and low- Mg^{2+} solution containing (mM): NaCl, 140; KCl, 5.4; $MgCl_2$, 0.5; $CaCl_2$, 0.2; KH_2PO_4, 1.2; taurine, 50; D-glucose, 5.5; Hepes–NaOH, 5; pH 6.9. Collagenase type II (224 U/ml, Worthington), elastase (1.9 U/ml, Worthington), protease (0.9 U/ml, Sigma Aldrich), and bovine serum albumin (BSA) 1 mg/ml were added. The digestion step was carried out for 20 min or 45 min, for atrial and SAN tissue, respectively, under gentle mechanical agitation at 37°C. Tissue strips were then washed out, and transferred into a modified 'Kraftbrühe' (KB) medium containing (mM): l-glutamic acid, 70; KCl, 20; KOH, 80; d-β-OH-butyric acid, 10; KH_2PO_4, 10; taurine, 10; BSA, 1 mg/ml; and Hepes–KOH, 10; pH 7.4. Single myocytes were manually dissociated in KB solution by employing a fire-polished glass pipette. Finally, extracellular Ca^{2+} concentration was recovered up to 1.3 mM. A drop of cell suspension was seeded onto sterilised laminin-coated coverslips. After 30-45 min, Tyrode solution containing 10% BSA was added, and cells were stored at 37°C until used in humidified 5% CO_2-95% air at 37^0C. All experiments were performed at room temperature.

Patch-clamp current recordings were performed with an Axopatch 200B amplifier (Axon Instruments) using fire-polished pipettes with a resistance of 3-4 MΩ pulled from

filamented borosilicated glass capillaries (Harvard Apparatus, 1.5 mm OD x 1.17 mm ID). Data were acquired and analysed by using a Digidata 1322A interface (Axon Instruments) and pCLAMP software (version 10, Axon Instruments). Action potentials were recorded in the current clamp mode. Cardiomyocytes were stimulated using a 5 ms current pulse. The resting membrane potential, the magnitude of the initial depolarisation and the action potential duration at which 50 and 90% repolarisation occurred were measured (APD_{50} and APD_{90} respectively). The cells were clamped at -60 mV in an extracellular solution containing (mM): NaCl 135, KCl 5.4, $CaCl_2$ 2, $MgCl_2$ 1, NaH_2PO_4 0.33, H-HEPES 5, Glucose 10 (buffered to pH 7.4 with NaOH). The intracellular solution was (mM): K gluconate 110, KCl 20, NaCl 10, $MgCl_2$ 1, MgATP 2, EGTA 2, Na_2GTP 0.3 (buffered to pH 7.2 with KOH). The liquid junction potential was +13 mV.

Measurement of atrial electrophysiology using multielectrode arrays

Using a multi-electrode array (MEA, Multichannel Systems), we investigated the effect of ablation of $G\alpha_{i2}$ on electrophysiological parameters in ex-vivo atrial tissue (33). Left atria were dissected from isolated mouse hearts after mounting in a Langendorff setup and perfused with Krebs solution supplemented with 30 mM 2, 3-butanedione monoxime. The tissue was then transferred to the array perfused with Krebs solution (37°C; 95% O2 / 5% CO2). Experiments were conducted in the absence and the presence of 10 nM – 10 µM carbachol. Left atrial electrophysiology was assessed during electrical stimulation using a multi-electrode array (MEA) system which allows non-invasive synchronous multifocal recording of extracellular field potentials. The MEA (MEA2100, Multichannel Systems, Reutlingen, Germany) consists of 60 microelectrodes arranged in an 8×8 matrix, with a 20 µm electrode diameter and an inter-electrode distance of 200 µm, Myocardial samples were positioned in the center of the MEA dish, held in contact with electrodes by a holder, and

continuously superfused with oxygenated Krebs solution at 37°C. Baseline electrical stimulation (bipolar pulses, 2x threshold, 2ms duration, 4 Hz frequency) was applied via one of the MEA microelectrodes. Field potential data were acquired simultaneously from all 60 microelectrodes. S1-S2 train stimulation with a S1-S1 cycle length of 250 ms was used to assess atrial effective refractory period (AERP). To assess conduction properties, isolated atria were sequentially stimulated (4 Hz) from one electrode of each 4 edges of the array. Field potential recordings obtained in these conditions were processed using LabChart7 (ADINSTRUMENTS, UK) to define local activation time based on minimum of the derivative of field potential. Average conduction velocity (CV) was calculated by linear regression relating inter electrode distance to activation times, as previously described (Opel et al., 2015). The slope of the regression line was the average conduction velocity (CV). Minimal wave-front cycle length (WFCL) was calculated for each isolated atria as AERPxCV.

Statistical Analysis

The mean and standard error of the mean are presented. Student's t-test or one way ANOVA was used, with a *P*-value < 0.05 being statistically significant.

Results

Inward currents in right and left atria

Using a step voltage protocol, current-voltage (I-V) relationships of atrial cardiomyocytes isolated from the right atria (RA) and left atria (LA) were compared in control mice (normal genotype littermates from the $G\alpha_{i2}$ crosses) (Figure 1). Currents were larger and showed greater inward rectification in RA than in the LA in the presence of carbachol (Figure 1 and 3). Experiments were also performed in the presence of GTPγS in the patch pipette to activate GIRK currents in the absence of receptor stimuation. In these experimental conditions, we still obtained a larger current in RA (-59.8 ± 6.5 pA/pF, n=5) compared to LA (-27.8 ± 2 pA/pF, n=5) of $G\alpha_{i2}$ (+/+) atrial myocytes .

In $G\alpha_{i2}$ (-/-) mice, the I/V relationship of the RA was altered with larger basal and carbachol-activated inward currents in the RA (Figure 2 and 4). In mice with the combined deletion of $G\alpha_{i1}/G\alpha_{i3}$ there were reduced carbachol-activated currents in the RA (Figure 3 and 4). The effects of $G\alpha_{i2}$ deletion were more pronounced in the RA, leading to loss of regional difference across the atria. Kinetics of GIRK current activation by carbachol were assesed using a twenty second application of agonist as we have previously described (2; 3; 31). There were no major changes in activation and rapid desensitisation between RA and LA and in the mice with either $G\alpha_{i2}$ or $G\alpha_{i1}/G\alpha_{i3}$ deletion (Table 1). In contrast, deactivation was slower in the RA than the LA but this pattern was not changed in the $G\alpha_{i2}$ (-/-) mice and in mice with combined $G\alpha_{i1}/G\alpha_{i3}$ deletion (Table 1).

We examined for expression changes of relevant components in the signalling cascade in the RA and LA of $G\alpha_{i2}$ (-/-) mice and littermate controls. Using quantitative real time reverse transcription PCR, we measured the expression of $G\alpha_{i1}$ (Gnai1), $G\alpha_{i3}$ (Gnai3),

some representative Gβγs (Gnb1, Gnb4, Gng7, Gng11) and the GIRK chanel subunits (Kcnj3 and Kcnj5) and the results are shown in Table 2. Gnb4 and Gng11 were chosen as they have potentially been associated with cardiovascular traits in particular heart rate in genome wide association studies (10). In general, the changes between $G\alpha_{i2}$ (-/-) mice and littermate controls are modest even when significant. However in $G\alpha_{i2}$ (-/-) mice GIRK channel subunit kcnj5 expression was increased in both atrial chambers suggesting that some of the differences in regulation of GIRK channels in $G\alpha_{i2}$ (-/-) mice may be related to transcriptional changes in channel expression.

Comparison with the SA node

We also isolated and patch clamped SA nodal cells. GIRK currents were of a similar magnitude as that in the RA but rectified more strongly and deactivated more rapidly after carbachol application (Figure 5 and Table 1). The properties of the currents in the SA node were unaffected in mice with global genetic deletion of $G\alpha_{i2}$ or $G\alpha_{i1}/G\alpha_{i3}$.

Single-cell action potentials

It might be predicted that an increased GIRK current in $G\alpha_{i2}$ (-/-) mice might lead to a shortened action potential duration and atrial effective refractory period. We compared atrial action potentials in the RA and LA myocytes in control and $G\alpha_{i2}$ (-/-) mice and, found that RA atrial myocytes from RA $G\alpha_{i2}$ (-/-) mice had a shorter APD_{90} than control RA myocytes. A similar trend was observed in the LA myocytes though this was not statisitically significant (Figure 6).

Carbachol (10μM) led to shortening of APD with a more pronounced effect in the RA. The decrease of the APD_{90} reached 61 ± 3 % in $G\alpha_{i2}$ (+/+) LA (n=9) and 76 ± 3 % in

$G\alpha_{i2}$ (+/+) RA (n= 8, p=0.006). In $G\alpha_{i2}$ (-/-) murine atrial myocytes, carbachol decreased APD_{90} by 57 ± 7% in the LA (n=7) and by 50 ± 8% in the RA (n=7, NS).

Tissue electrophysiology

We performed an analysis of the tissue electrophysiology in isolated left atria using a multielectrode array. The analysis of intact right atria was complicated by the intrinsic pacemaking activity. In the $G\alpha_{i2}$ (-/-) LA, there was a shortened effective refractory period (ERP), and no alteration in conduction velocity in comparison to $G\alpha_{i2}$ (+/+) LA, resulting in a significant decrease in potential path length for re-entry (Figure 7). A similar relative decrease of left atrial ERP was observed in the presence of carbachol (10 nM to 10 μM) between $G\alpha_{i2}$ (-/-) and control, with no significant difference in log EC_{50}, i.e. -6.9 +/- 0.4 vs -7.1 +/- 0.4 respectively. Carbachol did not alter left atrial CV (Figure 7).

Discussion

Our main findings are that in murine atria specific isoforms of inhibitory G-proteins have defined roles in controlling GIRK channel function. Specifically $G\alpha_{i2}$ suppresses the basal and agonist induced activity of GIRK whilst $G\alpha_{i1}$ and\or $G\alpha_{i3}$ mediate muscarinic activation of the current. Our experiments are in agreement with previous work, showing larger GIRK currents in the RA and the SAN regions compared to the LA region (12; 13; 23; 26; 40). Deletion of $G\alpha_{i2}$ accentuated this chamber asymmetry whilst it was attenuated in mice with global genetic deletion of $G\alpha_{i1}$ and $G\alpha_{i3}$. In keeping with the changes in GIRK currents, the global genetic deletion of $G\alpha_{i2}$ resulted in a shortened action potential duration, reduced tissue atrial effective refractory period and reduced minimum wave front cycle length.

These findings complement our previous work in which we have investigated heart rate regulation in various G-protein alpha subunit knockout mice (41; 46). Specifically mice with global and SA node specific deletion of $G\alpha_{i2}$ were tachycardic with impaired high frequency responses in heart rate variability studies. It is worth stating that the majority of studies reported here were conducted in the atria and reveal differences between the SA node and across the atria in GIRK channel signalling and G-protein dependency. Our observations reported here in the SA node show preserved signalling via muscarinic receptors to GIRK channels with deletion of both $G\alpha_{i2}$ and combined $G\alpha_{i1}$\$G\alpha_{i3}$. This suggests that GIRK channel independent mechanisms may be important in determining the *in-vivo* phenotype in $G\alpha_{i2}$ knockout mice. Specifically the loss of negative coupling to adenylate cyclase, fall in cAMP and effects on the hyperpolarization activated cyclic nucleotide gated channel and\or modulation of protein kinase A regulating the "calcium clock" may be important (20).

Inhibitory G-protein α subunits and GIRK channel function

GIRK channels are traditionally viewed as an example of a canonical effector activated by Gβγ subunits. However it is clear that Gα subunits play a role. For example, we demonstrated in heterologous systems that channel activation seemed to be preferentially activated via inhibitory rather than stimulatory G-proteins (21). Furthermore, studies have shown that the inhibitory G-protein heterotrimer can bind to the channel complex (6; 9; 37). This interaction may have important functional consequences namely that it surpresses basal current activity (6; 34). In other studies the Dascal laboratory demonstrated that there may be isoform differences in the nature of this behaviour between $G\alpha_{i1}$ and $G\alpha_{i3}$ (15). One issue with a proportion of this work is that the conclusions often depend on overexpression of engineered components in heterologous expression systems. It is unclear whether these kinds of effect occur in native settings with physiological levels of G-protein and channel expression. In this study in native atrial myocytes we show that deletion of $G\alpha_{i2}$ leads to an unexpected increase in basal and agonist activated currents. One interpretation of this finding is that inhibitory G-protein α subunits do indeed have an ability in-vivo to negatively regulate GIRK currents. However, our data reveal another potential mechanism namely transcriptional changes in GIRK channel subunit expression engendered by $G\alpha_{i2}$ deletion. Specifically in the $G\alpha_{i2}$ (-/-) mice, expression levels for kcnj3 and kcnj5 mRNA, in a statistically significant fashion for the latter, were increased compared to littermate controls and the magnitude of these effects were comparable to the changes in GIRK current density observed. In contrast, combined deletion of $G\alpha_{i1}$ and $G\alpha_{i3}$ impairs the magnitude of muscarinic activation sugessting that one of $G\alpha_{i1}$ and $G\alpha_{i3}$ or both is important for mediating the agonist induced response. Although we studied single isolated cardiac cells *ex-vivo*, it is still possible that extracardiac effects could lead to long lasting changes in myocyte biology.

We also examined if deletion of $G\alpha_{i2}$ had effects on the expression of other components in the signalling cascade namely Gnai1, Gnai3, Gnb1, Gnb4, Gng7 and Gng11. These experiments have substantial practical complications as there are five G-protein beta genes and fourteen G-protein gamma genes. We selected four to examine for compensatory changes in part determined from genome wide association studies in heart rate and our own unpublished studies (10). Whilst there were some changes these were modest in magnitude (possible decreases in expression of gnb1 and gng11 in the LA but no significant change change in gnb4, gng7, gnai1 or gnai3). Furthermore, in the functional studies in $G\alpha_{i2}$ (-/-) mice, carbachol led to increased agonist induced current activation suggesting $G_{\beta\gamma}$ expression was not limiting for signal transduction.

Regional differences

There were regional differences in the nature and coupling profile of GIRK currents in supraventricular tissues. GIRK currents were larger in the right atrium and SA node and these differences were accentuated in the right atrium by global genetic deletion of $G\alpha_{i2}$. Kinetic analysis also showed that GIRK current inactivation is faster in the RA and the SAN regions compared to the left atrium. This fast inactivation of the GIRK currents in the RA and pacemaker regions could reflect differential expression of regulators of G-protein signalling that can increase the hydrolysis rate of GTP bound and active G-protein α subunits (4; 33; 36). Furthermore, GIRK currents were more outwardly rectifying in the SA node and this could contribute to their importance in recovery of heart rate after exercise as explored recently in GIRK4 knockout mice as they may play a more significant role at depolarised potentials (30).

Another interesting finding is that the molecular details of the signalling system differ between closely related regions of the heart. So whilst $G\alpha_{i2}$ and $G\alpha_{i1}\backslash G\alpha_{i3}$ seem to have roles

in inhibition and activation respectively in the atria this pattern does not exist in the SA node. Indeed, a significant amount of redundancy is suggested as GIRK channel activation was little affected in both $G\alpha_{i2}$ and $G\alpha_{i1}\backslash G\alpha_{i3}$ knockout mice. This suggests that the specifics of the signalling can be tissue and region dependent. G-protein deletion had no effect on the kinetics of signalling suggesting that this was predominantly determined by other factors such as the expression of regulators of G-protein signalling.

G-protein deletion and predisposition to arrhythmia

The increase in GIRK currents in mice with global genetic deletion of $G\alpha_{i2}$ might lead to more general effects on single cell and tissue level electrophysiology. Indeed, the increase GIRK currents was sufficient to decrease the action potential duration. Furthermore, in whole left atrial preparations, $G\alpha_{i2}$ shortened the atrial effective refractory period without an effect on conduction velocity leading to a decrease minimum wave front cycle length. This change would be potentially proarrhythmic. We have also previously observed that $G\alpha_{i2}$ deletion in the ventricle and silencing of the vagal input increases the predisposition to ventricular arrhythmia (28; 47). The mechanism is different with an effect on calcium channel regulation and expression (47). It is also known that GIRK4 knockout mice are resistant to the induction of atrial fibrillation whilst RGS6 knockout mice with increased GIRK channel activity are predisposed (18; 36). Other investigators have observed in the dog that $G\alpha_{i2}$ and\or $G\alpha_{i3}$ knockdown using cell permeable peptides may surpress vagally mediated atrial fibrillation when delivered into the posterior left atrium (1). The authors did not examine the specifics of the mechanism and whether it was related to GIRK channel activation.

Action potential duration has been shown to decrease with increasing distance from the SAN region (26; 32). In contrast, GIRK currents are larger in the right atrium than left

atrium and this suggests there are other important electrophysiological determinants of the variation in action potential duration across the atria. The shortened action potential duration in the left atrium is potentially important as it may allow the support of higher frequency rotors in and around the pulmonary veins (40) though in this study the authors found higher GIRK currents in the left versus right atrium of sheep. Despite this lack of consensus, suppression of GIRK channel activity in the left atrium abrogates re-entry and atrial fibrillation (8).

Conclusions

Whilst not directly addressing the issue our studies are compatible with the long standing view that Gβγ subunits are important for GIRK channel activation. However they do reveal layers of complexity in how the Gα heterotrimeric G-protein subunit might shape this response. A body of work, which we discuss above, has suggested various ways by which this might occur including direct protein-protein interaction between G-protein heterotrimer components and channels domains. However much of this work is accomplished by expressing components, often at non-physiological levels, in model cell systems. Here we examine native signalling in various chambers and regions of the heart using mice with global genetic deletion of Gα subunits. Our overall conclusion is that there is much plasticity in the system with the exact importance of a specific Gα subunit being dependent on tissue region expression. Gα subunits may directly suppress GIRK currents in native systems but this could be accounted for by additional effects on channel transcription. These observed phenomena may result from variations in Gα subunit expression or compartmentation with the channel in different cardiac regions and these are topics for future investigation.

Acknowledgements

We thank the British Heart Foundation (RG/15/15/31742) and the Intramural Research Program of the NIH (project Z01ES101643) for funding this research. D.M. was supported by a grant from la Fédération Française de Cardiologie. The authors have no conflicts of interest to declare.

Reference List

1. **Aistrup GL, Villuendas R, Ng J, Gilchrist A, Lynch TW, Gordon D, Cokic I, Mottl S, Zhou R, Dean DA, Wasserstrom JA, Goldberger JJ, Kadish AH and Arora R**. Targeted G-protein inhibition as a novel approach to decrease vagal atrial fibrillation by selective parasympathetic attenuation. *Cardiovasc Res* 83: 481-492, 2009.

2. **Benians A, Leaney JL, Milligan G and Tinker A**. The dynamics of formation and action of the ternary complex revealed in living cells using a G-protein-gated K+ channel as a biosensor. *J Biol Chem* 278: 10851-10858, 2003.

3. **Benians A, Leaney JL and Tinker A**. Agonist unbinding from receptor dictates the nature of deactivation kinetics of G-protein gated K+ channels. *Proc Natl Acad Sci U S A* 100: 6239-6244, 2003.

4. **Benians A, Nobles M, Hosny S and Tinker A**. Regulators of G-protein signalling form a quaternary complex with the agonist, receptor and G-protein: a novel explanation for the acceleration of signalling activation kinetics. *J Biol Chem* 280: 13383-13394, 2005.

5. **Berlin S, Keren-Raifman T, Castel R, Rubinstein M, Dessauer CW, Ivanina T and Dascal N**. G alpha(i) and G betagamma jointly regulate the conformations of a G betagamma effector, the neuronal G protein-activated K+ channel (GIRK). *J Biol Chem* 285: 6179-6185, 2010.

6. **Berlin S, Tsemakhovich VA, Castel R, Ivanina T, Dessauer CW, Keren-Raifman T and Dascal N**. Two distinct aspects of coupling between Galpha(i) protein and G protein-activated K+ channel (GIRK) revealed by fluorescently labeled Galpha(i3) protein subunits. *J Biol Chem* 286: 33223-33235, 2011.

7. **Bettahi I, Marker CL, Roman MI and Wickman K**. Contribution of the Kir3.1 subunit to the muscarinic-gated atrial potassium channel IKACh. *J Biol Chem* 277: 48282-48288, 2002.

8. **Bingen BO, Neshati Z, Askar SF, Kazbanov IV, Ypey DL, Panfilov AV, Schalij MJ, de Vries AA and Pijnappels DA**. Atrium-specific Kir3.x determines inducibility, dynamics, and termination of fibrillation by regulating restitution-driven alternans. *Circulation* 128: 2732-2744, 2013.

9. **Clancy SM, Fowler CE, Finley M, Suen KF, Arrabit C, Berton F, Kosaza T, Casey PJ and Slesinger PA**. Pertussis-toxin-sensitive Galpha subunits selectively bind to C-terminal domain of neuronal GIRK channels: evidence for a heterotrimeric G-protein-channel complex. *Mol Cell Neurosci* 28: 375-389, 2005.

10. **den Hoed M, Eijgelsheim M, Esko T, Brundel BJ, Peal DS, Evans DM, Nolte IM, Segre AV, Holm H, Handsaker RE, Westra HJ, Johnson T, Isaacs A, Yang J, Lundby A, Zhao JH, Kim YJ, Go MJ, Almgren P, Bochud M, Boucher G, Cornelis MC, Gudbjartsson D, Hadley D, van der Harst P, Hayward C, den HM, Igl W, Jackson AU, Kutalik Z, Luan J, Kemp JP, Kristiansson K, Ladenvall C, Lorentzon M, Montasser ME, Njajou OT, O'Reilly PF, Padmanabhan S, St PB, Rankinen T, Salo P, Tanaka T, Timpson NJ, Vitart V, Waite L, Wheeler W,**

Zhang W, Draisma HH, Feitosa MF, Kerr KF, Lind PA, Mihailov E, Onland-Moret NC, Song C, Weedon MN, Xie W, Yengo L, Absher D, Albert CM, Alonso A, Arking DE, de Bakker PI, Balkau B, Barlassina C, Benaglio P, Bis JC, Bouatia-Naji N, Brage S, Chanock SJ, Chines PS, Chung M, Darbar D, Dina C, Dorr M, Elliott P, Felix SB, Fischer K, Fuchsberger C, de Geus EJ, Goyette P, Gudnason V, Harris TB, Hartikainen AL, Havulinna AS, Heckbert SR, Hicks AA, Hofman A, Holewijn S, Hoogstra-Berends F, Hottenga JJ, Jensen MK, Johansson A, Junttila J, Kaab S, Kanon B, Ketkar S, Khaw KT, Knowles JW, Kooner AS, Kors JA, Kumari M, Milani L, Laiho P, Lakatta EG, Langenberg C, Leusink M, Liu Y, Luben RN, Lunetta KL, Lynch SN, Markus MR, Marques-Vidal P, Mateo L, I, McArdle WL, McCarroll SA, Medland SE, Miller KA, Montgomery GW, Morrison AC, Muller-Nurasyid M, Navarro P, Nelis M, O'Connell JR, O'Donnell CJ, Ong KK, Newman AB, Peters A, Polasek O, Pouta A, Pramstaller PP, Psaty BM, Rao DC, Ring SM, Rossin EJ, Rudan D, Sanna S, Scott RA, Sehmi JS, Sharp S, Shin JT, Singleton AB, Smith AV, Soranzo N, Spector TD, Stewart C, Stringham HM, Tarasov KV, Uitterlinden AG, Vandenput L, Hwang SJ, Whitfield JB, Wijmenga C, Wild SH, Willemsen G, Wilson JF, Witteman JC, Wong A, Wong Q, Jamshidi Y, Zitting P, Boer JM, Boomsma DI, Borecki IB, van Duijn CM, Ekelund U, Forouhi NG, Froguel P, Hingorani A, Ingelsson E, Kivimaki M, Kronmal RA, Kuh D, Lind L, Martin NG, Oostra BA, Pedersen NL, Quertermous T, Rotter JI, van der Schouw YT, Verschuren WM, Walker M, Albanes D, Arnar DO, Assimes TL, Bandinelli S, Boehnke M, de Boer RA, Bouchard C, Caulfield WL, Chambers JC, Curhan G, Cusi D, Eriksson J, Ferrucci L, van Gilst WH, Glorioso N, de GJ, Groop L, Gyllensten U, Hsueh WC, Hu FB, Huikuri HV, Hunter DJ, Iribarren C, Isomaa B, Jarvelin MR, Jula A,

Kahonen M, Kiemeney LA, van der Klauw MM, Kooner JS, Kraft P, Iacoviello L, Lehtimaki T, Lokki ML, Mitchell BD, Navis G, Nieminen MS, Ohlsson C, Poulter NR, Qi L, Raitakari OT, Rimm EB, Rioux JD, Rizzi F, Rudan I, Salomaa V, Sever PS, Shields DC, Shuldiner AR, Sinisalo J, Stanton AV, Stolk RP, Strachan DP, Tardif JC, Thorsteinsdottir U, Tuomilehto J, van Veldhuisen DJ, Virtamo J, Viikari J, Vollenweider P, Waeber G, Widen E, Cho YS, Olsen JV, Visscher PM, Willer C, Franke L, Erdmann J, Thompson JR, Pfeufer A, Sotoodehnia N, Newton-Cheh C and Ellinor PT. Identification of heart rate-associated loci and their effects on cardiac conduction and rhythm disorders. *Nat Genet* 45: 621-631, 2013.

11. **Hibino H, Inanobe A, Furutani K, Murakami S, Findlay I and Kurachi Y**. Inwardly rectifying potassium channels: their structure, function, and physiological roles. *Physiol Rev* 90: 291-366, 2010.

12. **Hirose M, Carlson MD and Laurita KR**. Cellular mechanisms of vagally mediated atrial tachyarrhythmia in isolated arterially perfused canine right atria. *J Cardiovasc Electrophysiol* 13: 918-926, 2002.

13. **Hirose M, Leatmanoratn Z, Laurita KR and Carlson MD**. Partial vagal denervation increases vulnerability to vagally induced atrial fibrillation. *J Cardiovasc Electrophysiol* 13: 1272-1279, 2002.

14. **Huang CL, Slesinger PA, Casey PJ, Jan YN and Jan LY**. Evidence that direct binding of G beta gamma to the GIRK1 G protein-gated inwardly rectifying K+ channel is important for channel activation. *Neuron* 15: 1133-1143, 1995.

15. **Ivanina T, Varon D, Peleg S, Rishal I, Porozov Y, Dessauer CW, Keren-Raifman T and Dascal N**. Galphai1 and Galphai3 differentially interact with, and regulate, the G protein-activated K+ channel. *J Biol Chem* 279: 17260-17268, 2004.

16. **Jiang M, Spicher K, Boulay G, Martin-Requero A, Dye CA, Rudolph U and Birnbaumer L**. Mouse gene knockout and knockin strategies in application to alpha subunits of Gi/Go family of G proteins. *Methods Enzymol* 344: 277-298, 2002.

17. **Kahr PC, Piccini I, Fabritz L, Greber B, Scholer H, Scheld HH, Hoffmeier A, Brown NA and Kirchhof P**. Systematic analysis of gene expression differences between left and right atria in different mouse strains and in human atrial tissue. *PLoS One* 6: e26389, 2011.

18. **Kovoor P, Wickman K, Maguire CT, Pu W, Gehrmann J, Berul CI and Clapham DE**. Evaluation of the role of I(KACh) in atrial fibrillation using a mouse knockout model. *J Am Coll Cardiol* 37: 2136-2143, 2001.

19. **Krapivinsky G, Gordon EA, Wickman K, Velimirovic B, Krapivinsky L and Clapham DE**. The G-protein-gated atrial K+ channel IKACh is a heteromultimer of two inwardly rectifying K(+)-channel proteins. *Nature* 374: 135-141, 1995.

20. **Lakatta EG, Maltsev VA and Vinogradova TM**. A coupled SYSTEM of intracellular Ca2+ clocks and surface membrane voltage clocks controls the timekeeping mechanism of the heart's pacemaker. *Circ Res* 106: 659-673, 2010.

21. **Leaney JL, Milligan G and Tinker A**. The G protein α subunit has a key role in determining the specificity of coupling to, but not the activation of G protein-gated inwardly rectifying K^+ channels. *J Biol Chem* 275: 921-929, 2000.

22. **Leaney JL and Tinker A**. The role of members of the pertussis toxin-sensitive family of G proteins in coupling receptors to the activation of the G protein-gated inwardly rectifying potassium channel. *Proc Natl Acad Sci U S A* 97: 5651-5656, 2000.

23. **Li N, Csepe TA, Hansen BJ, Sul LV, Kalyanasundaram A, Zakharkin SO, Zhao J, Guha A, Van Wagoner DR, Kilic A, Mohler PJ, Janssen PM, Biesiadecki BJ, Hummel JD, Weiss R and Fedorov VV**. Adenosine-Induced Atrial Fibrillation: Localized Reentrant Drivers in Lateral Right Atria due to Heterogeneous Expression of Adenosine A1 Receptors and GIRK4 Subunits in the Human Heart. *Circulation* 134: 486-498, 2016.

24. **Liu GX, Derst C, Schlichthorl G, Heinen S, Seebohm G, Bruggemann A, Kummer W, Veh RW, Daut J and Preisig-Muller R**. Comparison of cloned Kir2 channels with native inward rectifier K+ channels from guinea-pig cardiomyocytes. *J Physiol* 532: 115-126, 2001.

25. **Logothetis DE, Kurachi Y, Galper J, Neer EJ and Clapham DE**. The beta gamma subunits of GTP-binding proteins activate the muscarinic K+ channel in heart. *Nature* 325: 321-326, 1987.

26. **Lomax AE, Rose RA and Giles WR**. Electrophysiological evidence for a gradient of G protein-gated K+ current in adult mouse atria. *Br J Pharmacol* 140: 576-584, 2003.

27. **Luscher C and Slesinger PA**. Emerging roles for G protein-gated inwardly rectifying potassium (GIRK) channels in health and disease. *Nat Rev Neurosci* 11: 301-315, 2010.

28. **Machhada A, Ang R, Ackland GL, Ninkina N, Buchman VL, Lythgoe MF, Trapp S, Tinker A, Marina N and Gourine AV**. Control of ventricular excitability by neurons of the dorsal motor nucleus of the vagus nerve. *Heart Rhythm* 12: 2285-2293, 2015.

29. **Mangoni ME, Traboulsie A, Leoni AL, Couette B, Marger L, Le QK, Kupfer E, Cohen-Solal A, Vilar J, Shin HS, Escande D, Charpentier F, Nargeot J and Lory P**. Bradycardia and slowing of the atrioventricular conduction in mice lacking CaV3.1/alpha1G T-type calcium channels. *Circ Res* 98: 1422-1430, 2006.

30. **Mesirca P, Marger L, Toyoda F, Rizzetto R, Audoubert M, Dubel S, Torrente AG, Difrancesco ML, Muller JC, Leoni AL, Couette B, Nargeot J, Clapham DE, Wickman K and Mangoni ME**. The G-protein-gated K+ channel, IKACh, is required for regulation of pacemaker activity and recovery of resting heart rate after sympathetic stimulation. *J Gen Physiol* 142: 113-126, 2013.

31. **Nobles M, Sebastian S and Tinker A**. HL-1 cells express an inwardly rectifying K+ current activated via muscarinic receptors comparable to that in mouse atrial myocytes. *Pflugers Arch* 460: 99-108, 2010.

32. **Nygren A, Lomax AE and Giles WR**. Heterogeneity of action potential durations in isolated mouse left and right atria recorded using voltage-sensitive dye mapping. *Am J Physiol Heart Circ Physiol* 287: H2634-H2643, 2004.

33. **Opel A, Nobles M, Montaigne D, Finlay M, Anderson N, Breckenridge R and Tinker A**. Absence of the Regulator of G-protein Signaling, RGS4, Predisposes to Atrial Fibrillation and Is Associated with Abnormal Calcium Handling. *J Biol Chem* 290: 19233-19244, 2015.

34. **Peleg S, Varon D, Ivanina T, Dessauer CW and Dascal N**. G(alpha)(i) controls the gating of the G protein-activated K(+) channel, GIRK. *Neuron* 33: 87-99, 2002.

35. **Pfaffinger PJ, Martin JM, Hunter DD, Nathanson NM and Hille B**. GTP-binding proteins couple cardiac muscarinic receptors to a K channel. *Nature* 317: 536-538, 1985.

36. **Posokhova E, Ng D, Opel A, Masuho I, Tinker A, Biesecker LG, Wickman K and Martemyanov KA**. Essential role of the m2R-RGS6-IKACh pathway in controlling intrinsic heart rate variability. *PLoS One* 8: e76973, 2013.

37. **Riven I, Iwanir S and Reuveny E**. GIRK channel activation involves a local rearrangement of a preformed G protein channel complex. *Neuron* 51: 561-573, 2006.

38. **Riven I, Kalmanzon E, Segev L and Reuveny E**. Conformational rearrangements associated with the gating of the G protein-coupled potassium channel revealed by FRET microscopy. *Neuron* 38: 225-235, 2003.

39. **Sakmann B, Noma A and Trautwein W**. Acetylcholine activation of single muscarinic K+ channels in isolated pacemaker cells of the mammalian heart. *Nature* 303: 250-253, 1983.

40. **Sarmast F, Kolli A, Zaitsev A, Parisian K, Dhamoon AS, Guha PK, Warren M, Anumonwo JM, Taffet SM, Berenfeld O and Jalife J**. Cholinergic atrial fibrillation: I(K,ACh) gradients determine unequal left/right atrial frequencies and rotor dynamics. *Cardiovasc Res* 59: 863-873, 2003.

41. **Sebastian S, Ang R, Abramowitz J, Weinstein LS, Chen M, Ludwig A, Birnbaumer L and Tinker A**. The in-vivo regulation of heart rate in the murine sinoatrial node by stimulatory and inhibitory heterotrimeric G-proteins. *Am J Physiol Regul Integr Comp Physiol* 305: 435-442, 2013.

42. **Slesinger PA, Reuveny E, Jan YN and Jan LY**. Identification of structural elements involved in G protein gating of the GIRK1 potassium channel. *Neuron* 15: 1145-1156, 1995.

43. **Wickman K, Nemec J, Gendler SJ and Clapham DE**. Abnormal heart rate regulation in GIRK4 knockout mice. *Neuron* 20: 103-114, 1998.

44. **Wickman KD, Iniguez Lluhl JA, Davenport PA, Taussig R, Krapivinsky GB, Linder ME, Gilman AG and Clapham DE**. Recombinant G-protein beta gamma-subunits activate the muscarinic-gated atrial potassium channel. *Nature* 368: 255-257, 1994.

45. **Zaritsky JJ, Redell JB, Tempel BL and Schwarz TL**. The consequences of disrupting cardiac inwardly rectifying K(+) current (I(K1)) as revealed by the targeted deletion of the murine Kir2.1 and Kir2.2 genes. *J Physiol* 533: 697-710, 2001.

46. **Zuberi Z, Birnbaumer L and Tinker A**. The role of inhibitory heterotrimeric G-proteins in the control of in-vivo heart rate dynamics. *Am J Physiol Regul Integr Comp Physiol* 295: R1822-R1830, 2008.

47. **Zuberi Z, Nobles M, Sebastian S, Dyson A, Shiang Y, Breckenridge RA, Birnbaumer L and Tinker A**. Absence of the inhibitory G-protein, $G\alpha_{i2}$, predisposes to ventricular cardiac arrhythmia. *Circ Arrhythm Electrophysiol* 3: 391-400, 2010.

Table Legends

Table 1. Deletion of $G\alpha_{i2}$ or $G\alpha_{i1/3}$ and GIRK currents kinetics across the atria. Cells were clamped at -60 mV and carbachol was applied for 20 ms with a fast perfusion system. Characteristics of the GIRK currents kinetics are presented in the table for the LA, RA and SAN region for the $G\alpha_{i2}$ (+/+), $G\alpha_{i2}$ (-/-), and $G\alpha_{i1/3}$ (-/-). The current inactivation characteristics (τdeac and lag inac) were faster in the RA and San compared to the LA (*$p<0.05$).

Table 2. Quantitative real-time reverse transcription PCR to measure gene expression in the RA and LA. Quantitative real-time reverse transcription PCR was performed as described in the Materials and Methods for the genes indicated in the Table. Measurements were performed in triplicate from $G\alpha_{i2}$ (-/-) mice (n=3) and littermate controls (n=3) (*$p<0.05$ using one way ANOVA).

Figure Legends

Figure 1. GIRK currents in the atrial tissue. A. Representative traces of currents measured in atrial myocytes isolated from the left and right atria of $G\alpha_{i2}$ (+/+) mice. B. Mean current-voltage relationships. Atrial myocytes were challenged with 10 μM carbachol. GIRK currents were larger in RA compared to LA.

Figure 2. Deletion of $G\alpha_{i2}$ affect the gradient of GIRK across the atria. Representative traces and mean current-voltage relationships of currents measured in atrial myocytes isolated from the left and right atria of $G\alpha_{i2}$ **(-/-)** mice. Basal GIRK currents were larger in RA compared to $G\alpha_{i2}$ **(+/+)**.

Figure 3. Deletion of $G\alpha_{i1/3}$ affect the gradient of GIRK across the atria. Representative traces and mean current-voltage relationships of currents measured in atrial myocytes isolated from the left and right atria of $G\alpha_{i1/3}$ (-/-) mice. There was a loss of GIRK current gradient between the LA and RA.

Figure 4. Comparison of GIRK currents in the LA and RA. Bar graph showing maximum GIRK currents measured at -120 mV. In $G\alpha_{i2}$ (+/+), carbachol (10 μM) led to a larger activation of GIRK currents in the RA. Deletion of Giα2 led to larger basal and carbachol-activated currents in the RA. Deletion of $G\alpha_{i1/3}$ led to smaller carbachol-activated currents in both LA and RA with a marked effect in the RA, thee consequence being a loss of gradient across the atria.

Figure 5. GIRK current in the SAN. Left panel: Representative traces of GIRK currents in control and after activation with 10 μM carbachol. Comparison is made between $G\alpha_{i2}$ **(+/+),** $G\alpha_{i2}$ (-/-) and $G\alpha_{i1/3}$ **(-/-).** Right panel: Mean current-voltage relationships. Atrial myocytes were challenged with 10 μM carbachol. GIRK currents were not affected by $G\alpha_i$ deletion.

Figure 6. Consequence of the deletion of $G\alpha_{i2}$ **on the action potential of single cardiomyocytes**. Single cardiomyocytes AP were measured after stimulation of cells by a 5 ms pulse after pacing at 1Hz for 60 seconds. The APD90 were longer in the RA, although the mean values did not reach significance when analyses with t-test due to the variability of the data values. Both APD50 and APD90 were significantly reduced in the $G\alpha_{i2}$ (-/-) right atria (* $p<0.05$).

Figure 7. **Electrophysiology of isolated right and left atria.** A) Atrial effective refractory period (ERP), (B) conduction velocity (CV) and (C) minimum wave front cycle length (mWFCL) in left atrial tissue deficient in $G\alpha_{i2}$ (-/-) mice compared to $G\alpha_{i2}$ (+/+) (* p-value <0.05). Dose-response for carbachol on left atrial AERP (D), relative AERP to baseline (E) and CV (F) in $G\alpha_{i2}$ (-/-) mice compared to $G\alpha_{i2}$ (+/+).

Table 1

	Gαi2 (+/+)			Gαi2 (-/-)			Gαi1/3 (-/-)		
	LA	**RA**	**SAN**	**LA**	**RA**	**SAN**	**LA**	**RA**	**SAN**
	N = 9	N=8	*N =10*	*N =12*	*N=10*	*N = 11*	N=7	N=8	*N=5*
Im, pA/pF	-85 ± 8	-86.5 ± 7.8	-55.9 ± 8	-77.6 ± 6.2	- 75.1± 7	-49.7 ± 6.2	-67 ± 4.2	-70± 9.5	-58.2 ± 18
GIRK, pA/pF	-106 ± 15	-162 ± 34.5	-108.3 ± 20	-87.8 ± 8.2	-128 ± 12	-118.3 ± 14.4	-92.51 ± 10	-134.8 ± 24	-175.2 ± 18
Lag + TTP, s	1.06 ± 0.06	0.84± 0.05	0.99 ± 0.01	0.9 ± 0.05	0.82 ± 0.04	0.96 ± 0.05	1 ± 0.05	0.68 ± 0.04	0.79 ± 0.07
tac , ms	188 ± 11.1	142 ± 11.3	162 ± 24.4	156 ± 10.8	153 ± 27	144 ± 7.2	256 ± 45	114 ± 13	143 ± 13.7
tdeac, ms	2996 ± 458	811 ± 66.6*	607 ± 92*	2654 ± 438	779± 137*	466 ± 40.3*	3567 ± 739	824 ± 141*	493 ± 71.3*
lag inac, s	0.68 ± 0.14	0.32 ± 0.06*	0.21± 0.01*	0.59 ± 0.08	0.33 ± 0.03*	0.23 ± 0.02*	0.53 ± 0.01	0.30 ± 0.07*	0.26 ± 0.01*
% des 20 s	25.8 ± 2.35	25.2 ± 3.34	20 ± 1.5	29.5 ± 3.4	27.1 ± 2.9	31 ± 3.2	22.5 ± 1.6	24.1 ± 2.7	14.1 ± 3.5
G	22.7 ± 1.3	18.7 ± 1	26.4 ± 2.7	25 ± 2.2	19.6 ± 1.3	22.8 ± 2.4	34.4 ± 3.3	22.6 ± 2.6	17.8 ± 2.2

Table 2

Genes	WT	KO	WT	KO
	LA	LA	RA	RA
	ΔCT	ΔCT	ΔCT	ΔCT
Gnai1	6.75 ± 0.06	6.98 ± 0.05	8.46 ± 0.35	8.15 ± 0.09
Gnai3	6.90 ± 0.18	6.65 ± 0.08	6.98 ± 0.12	7.42± 0.09
Gnb1	4.76 ± 0.14	5.72 ± 0.25*	5.21 ± 0.50	5.50 ± 0.07
Gnb4	7.98 ± 0.18	7.72 ± 0.07	8.75 ± 0.18	8.60 ± 0.08
Gng7	10.8 ± 0.14	11.5 ± 0.14	11.5 ± 0.51	11.7 ± 0.16
Gng11	7.04 ± 0.11	7.49 ± 0.03*	7.56 ± 0.21	7.43 ± 0.04
Kcnj3	2.86 ± 0.14	2.30 ± 0.07	3.62 ± 0.18	3.00 ± 0.05
Kcnj5	5.38 ± 0.12	4.86 ± 0.06*	5.51 ± 0.24	4.94 ± 0.07*

Figure 1

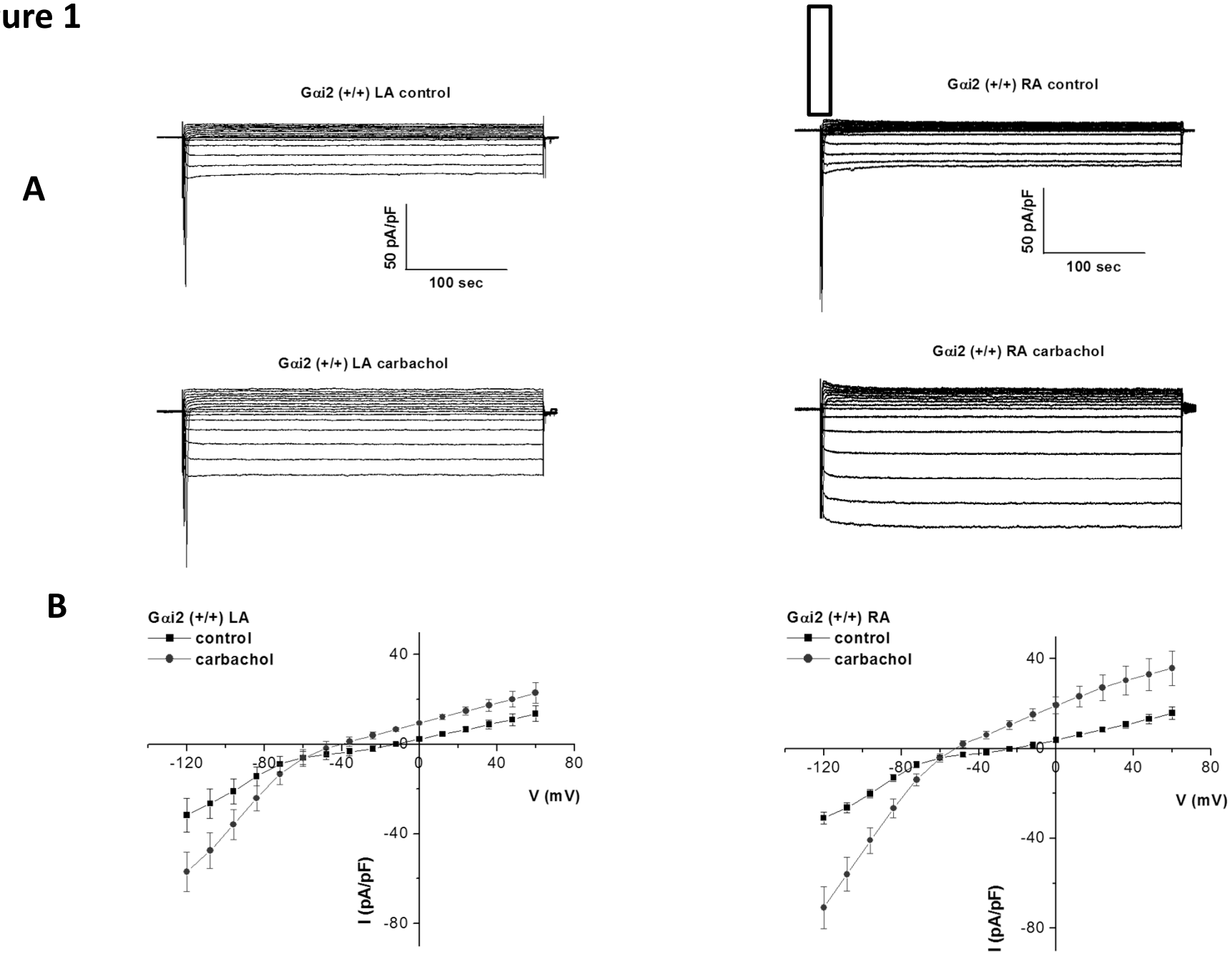
A
Gαi2 (+/+) LA control
50 pA/pF
100 sec
Gαi2 (+/+) RA control
50 pA/pF
100 sec
Gαi2 (+/+) LA carbachol
Gαi2 (+/+) RA carbachol
B
Gαi2 (+/+) LA
control
carbachol
40
0
-40
-80
-120
-80
-40
0
40
80
V (mV)
I (pA/pF)
Gαi2 (+/+) RA
control
carbachol
40
0
-40
-80
-120
-80
-40
0
40
80
V (mV)
I (pA/pF)

Figure 2

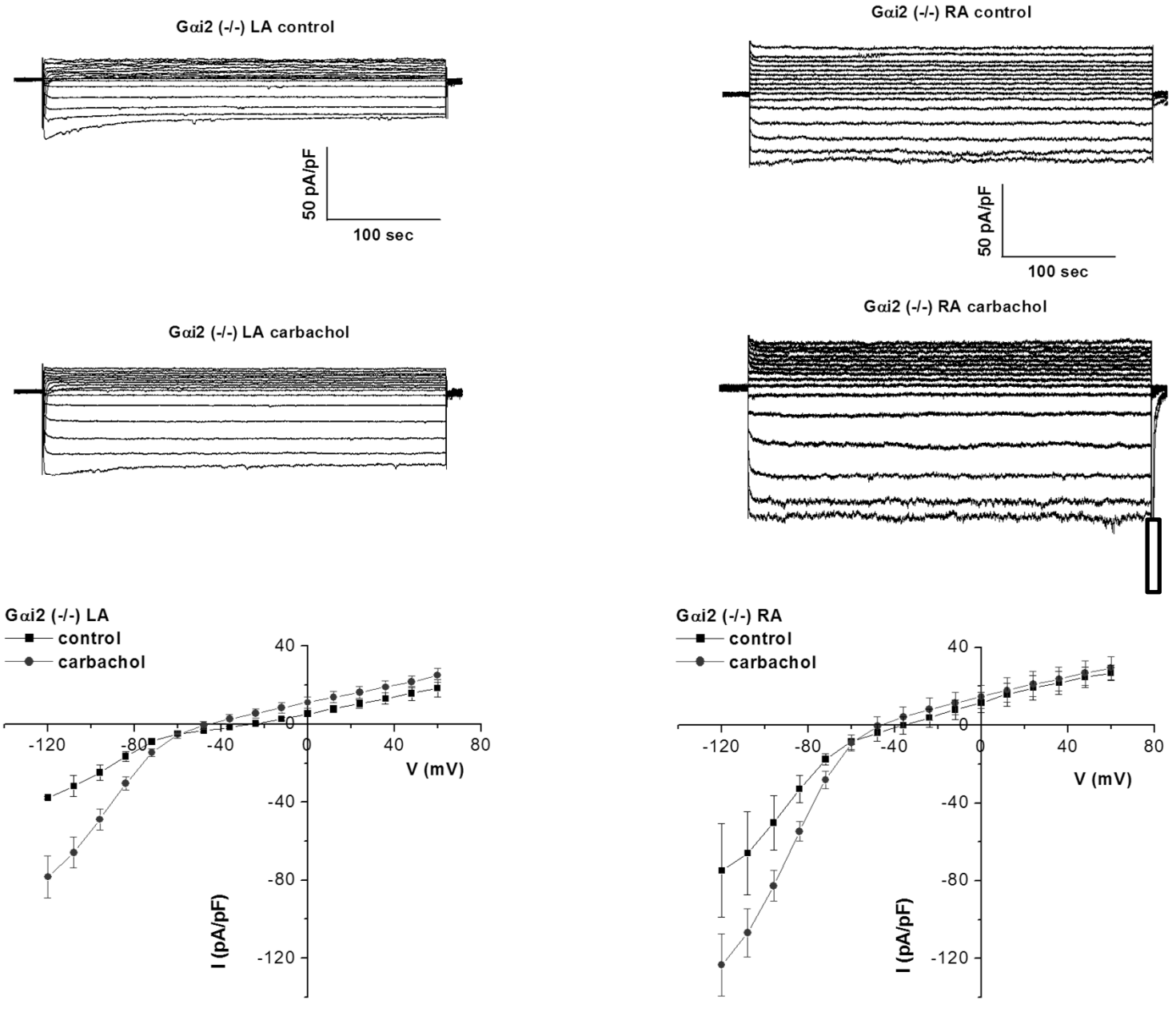
Gαi2 (-/-) LA control
50 pA/pF
100 sec
Gαi2 (-/-) RA control
50 pA/pF
100 sec
Gαi2 (-/-) LA carbachol
Gαi2 (-/-) RA carbachol
Gαi2 (-/-) LA
control
carbachol
V (mV)
I (pA/pF)
Gαi2 (-/-) RA
control
carbachol
V (mV)
I (pA/pF)

Figure 3

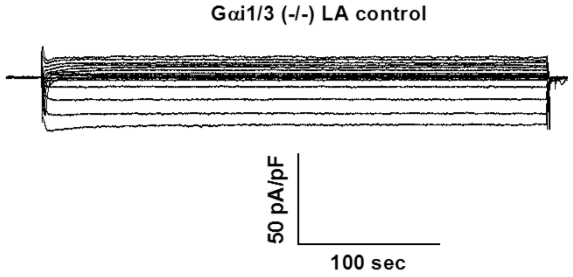
Gαi1/3 (-/-) LA control
50 pA/pF
100 sec

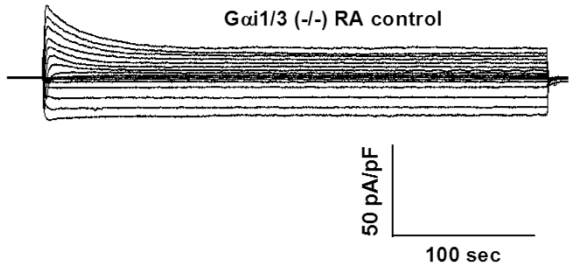
Gαi1/3 (-/-) RA control
50 pA/pF
100 sec

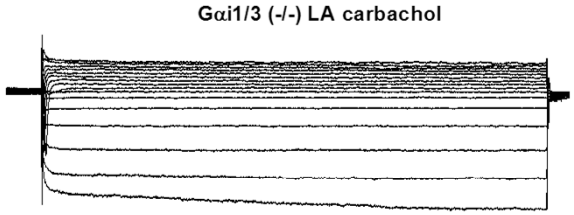
Gαi1/3 (-/-) LA carbachol

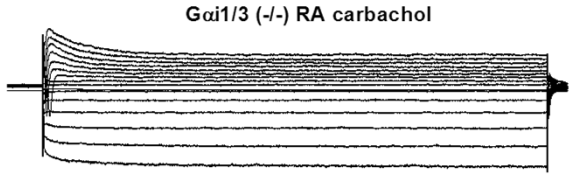
Gαi1/3 (-/-) RA carbachol

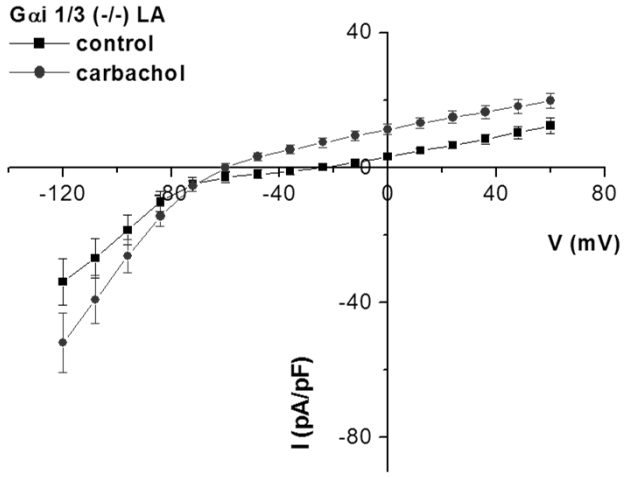
Gαi 1/3 (-/-) LA
control
carbachol
40
0
-40
-80
-120
-80
-40
0
40
80
V (mV)
I (pA/pF)

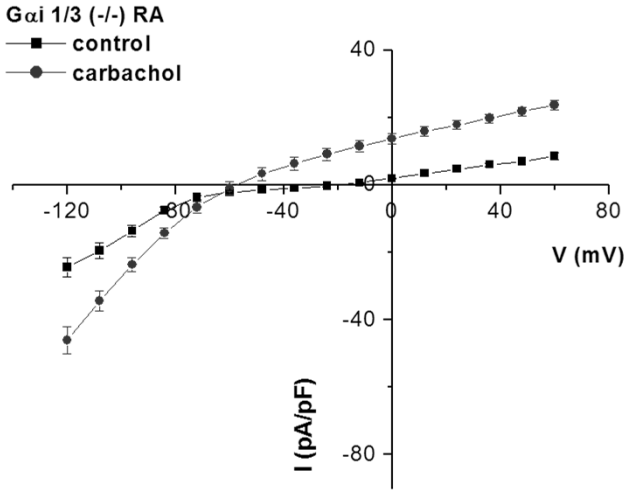
Gαi 1/3 (-/-) RA
control
carbachol
40
0
-40
-80
-120
-80
-40
0
40
80
V (mV)
I (pA/pF)

Figure 4

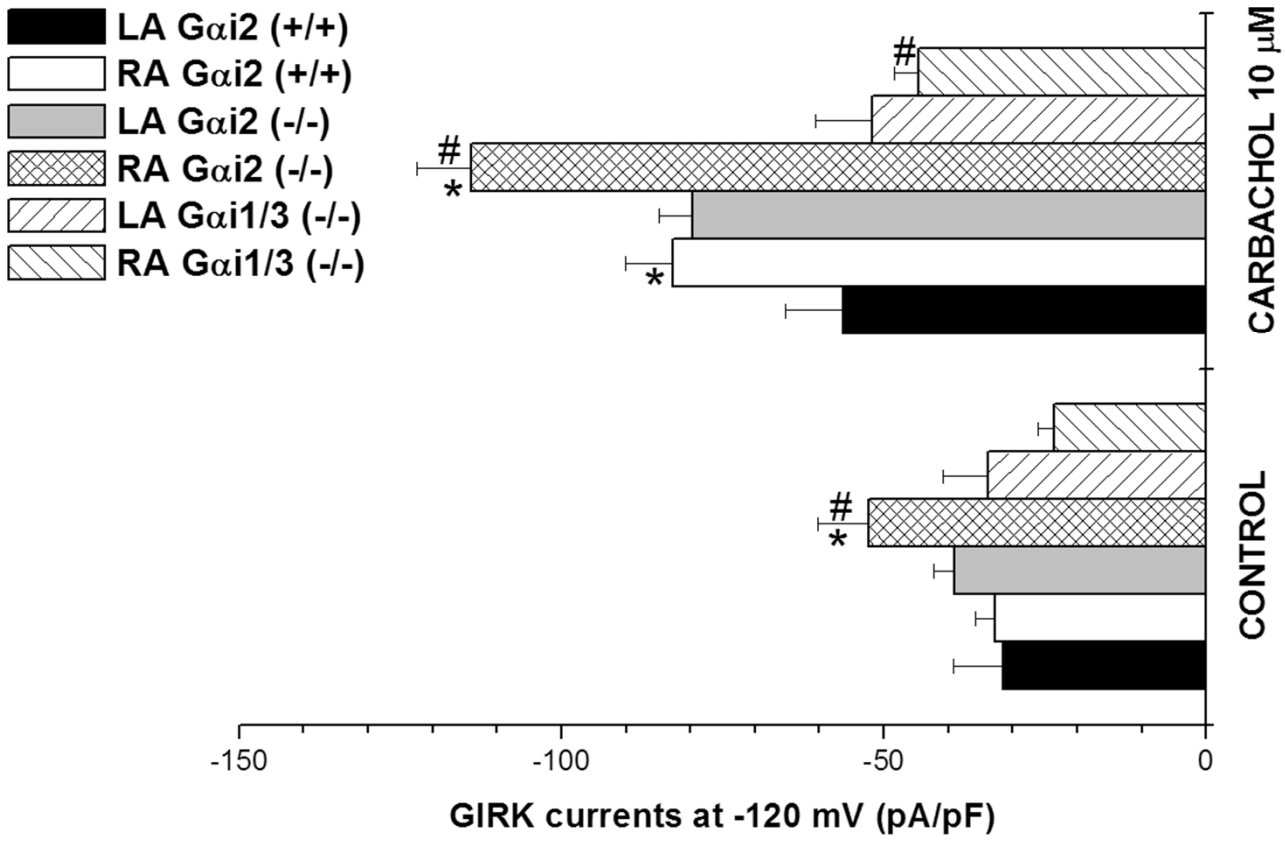
LA Gαi2 (+/+)
RA Gαi2 (+/+)
LA Gαi2 (-/-)
RA Gαi2 (-/-)
LA Gαi1/3 (-/-)
RA Gαi1/3 (-/-)
CARBACHOL 10 μM
CONTROL
#
*
-150
-100
-50
0
GIRK currents at -120 mV (pA/pF)

Figure 5

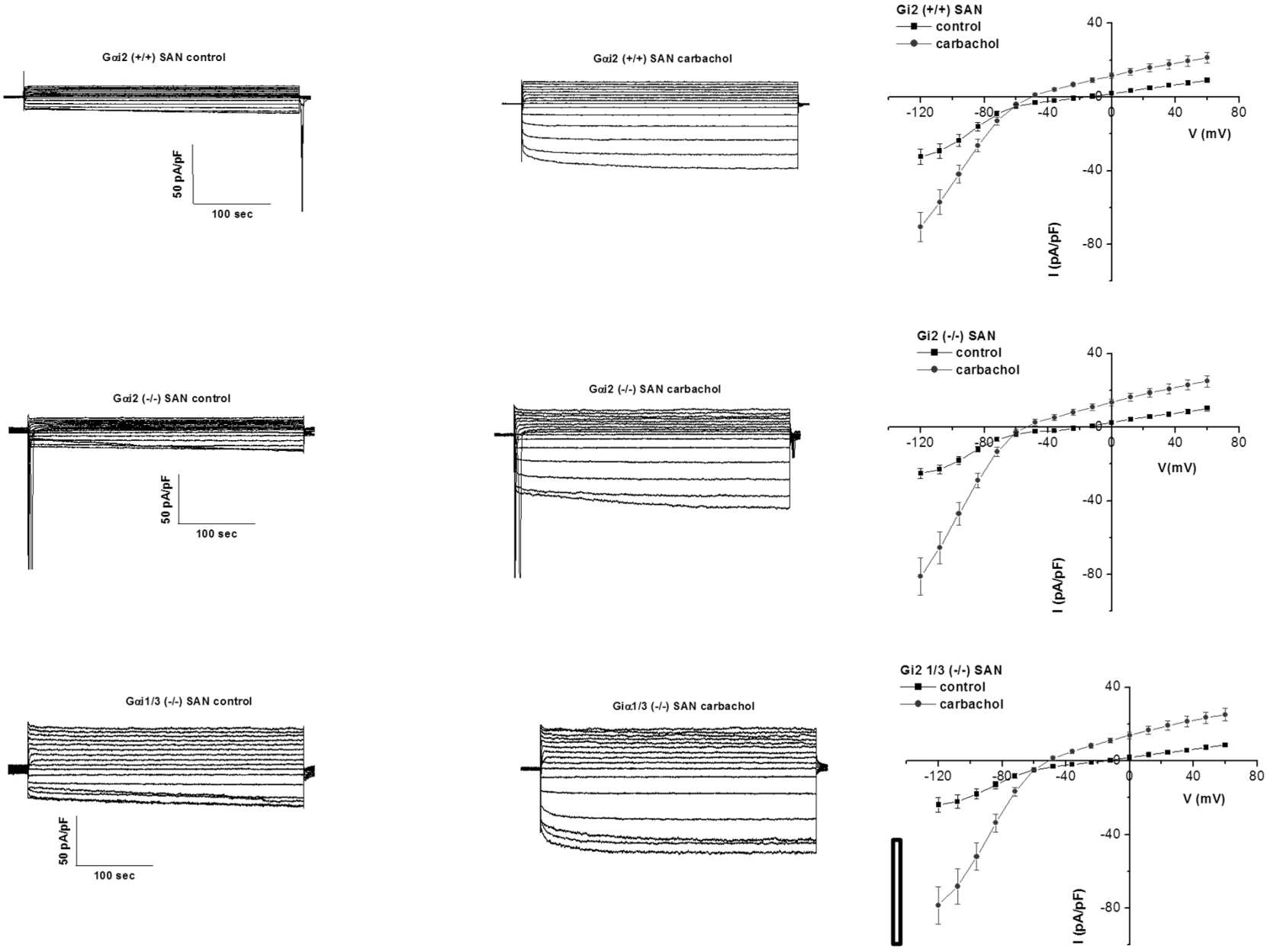
Gαi2 (+/+) SAN control
50 pA/pF
100 sec
Gαi2 (+/+) SAN carbachol
Gi2 (+/+) SAN
control
carbachol
40
0
-40
-80
-120
-80
-40
0
40
80
V (mV)
I (pA/pF)
Gαi2 (-/-) SAN control
50 pA/pF
100 sec
Gαi2 (-/-) SAN carbachol
Gi2 (-/-) SAN
control
carbachol
V(mV)
I (pA/pF)
Gαi1/3 (-/-) SAN control
50 pA/pF
100 sec
Giα1/3 (-/-) SAN carbachol
Gi2 1/3 (-/-) SAN
control
carbachol
V (mV)
I (pA/pF)

Figure 6

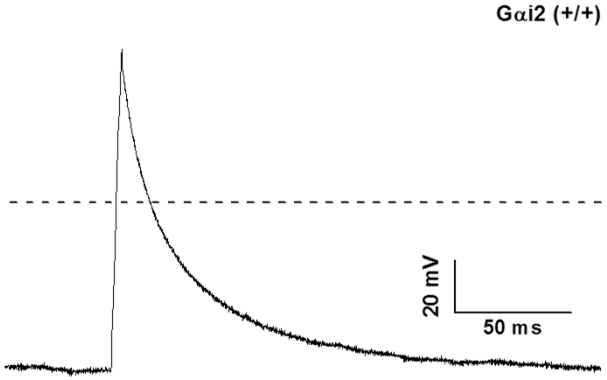

N=9
APD 50 = 20.3 ± 2.2 ms
APD 90 = 60 ± 7.3 ms

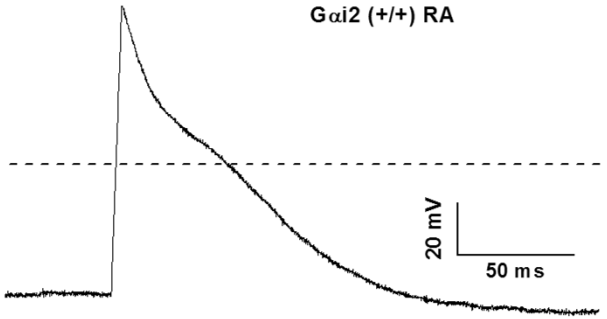

N=8
APD 50 = 21.5 ± 3.1 ms
APD 90 = 67.5 ± 8.7 ms

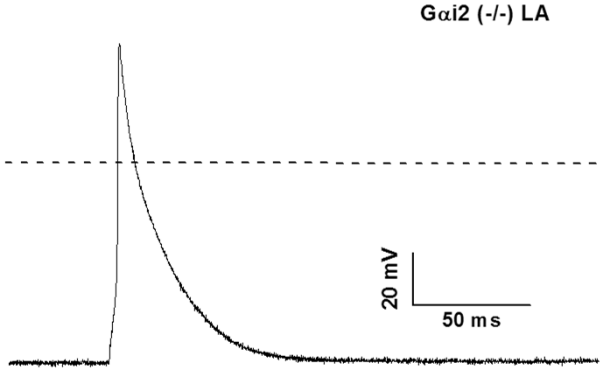

N=6
APD 50 = 16 ±2. 1 ms
APD 90 = 51 ± 7.4 ms

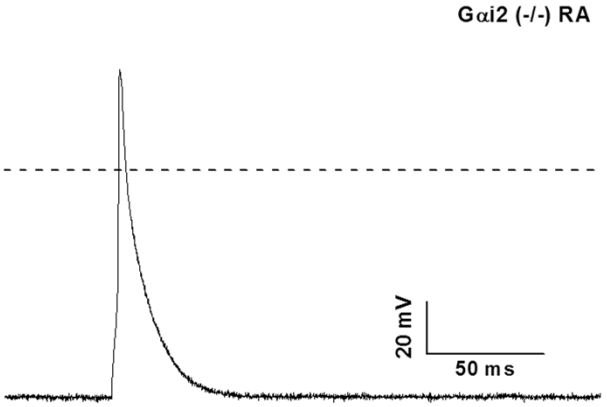

N=6
APD 50 = 11.4 ± 1.6 ms
APD 90 = 34.1 ± 7.1 ms

Figure 7

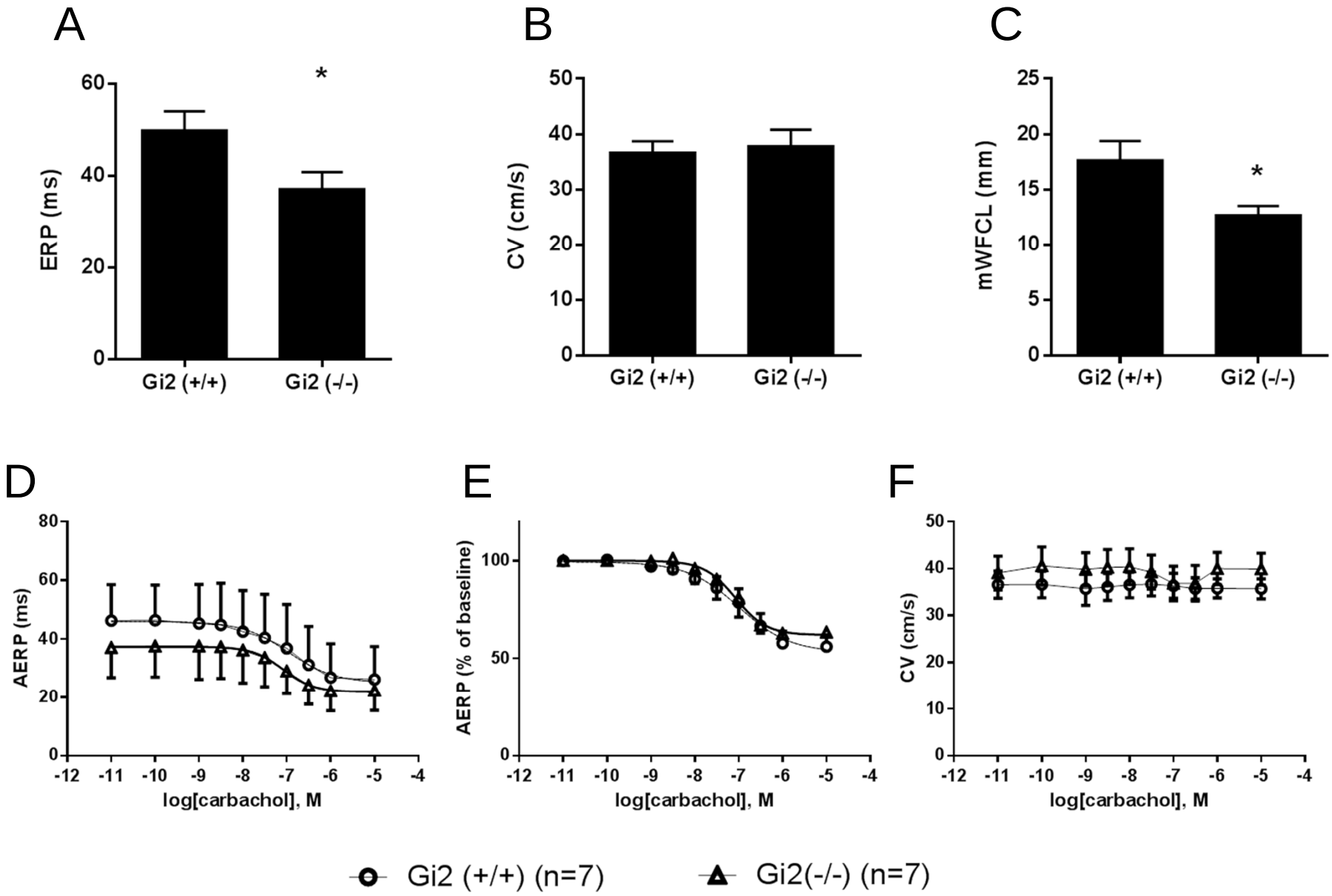
A
B
C
ERP (ms)
CV (cm/s)
mWFCL (mm)
Gi2 (+/+)
Gi2 (-/-)
*
D
E
F
AERP (ms)
AERP (% of baseline)
log[carbachol], M
Gi2 (+/+) (n=7)
Gi2(-/-) (n=7)